Variation in Summer Surface Air Temperature over Northeast Asia and Its Associated Circulation Anomalies

Wei CHEN[1], Xiaowei HONG[1,2], Riyu LU*[1], Aifen JIN[3], Shizhu JIN[3], Jae-Cheol NAM[4], Jin-Ho SHIN[4], Tae-Young GOO[4], and Baek-Jo KIM[4]

[1]*State Key Laboratory of Numerical Modeling for Atmospheric Sciences and Geophysical Fluid Dynamics, Institute of Atmospheric Physics, Chinese Academy of Sciences, Beijing* 100029

[2]*University of Chinese Academy of Sciences, Beijing* 100049

[3]*Department of Geography, Yanbian University, Yanji* 133002

[4]*National Institute of Meteorological Research, Korea Meteorological Administration, Jeju, Korea*

(Received 15 February 2015; revised 22 June 2015; accepted 26 June 2015)

ABSTRACT

This study investigates the interannual variation of summer surface air temperature over Northeast Asia (NEA) and its associated circulation anomalies. Two leading modes for the temperature variability over NEA are obtained by EOF analysis. The first EOF mode is characterized by a homogeneous temperature anomaly over NEA and therefore is called the NEA mode. This anomaly extends from southeast of Lake Baikal to Japan, with a central area in Northeast China. The second EOF mode is characterized by a seesaw pattern, showing a contrasting distribution between East Asia (specifically including the Changbai Mountains in Northeast China, Korea, and Japan) and north of this region. This mode is named the East Asia (EA) mode. Both modes contribute equivalently to the temperature variability in EA.

The two leading modes are associated with different circulation anomalies. A warm NEA mode is associated with a positive geopotential height anomaly over NEA and thus a weakened upper-tropospheric westerly jet. On the other hand, a warm EA mode is related to a positive height anomaly over EA and a northward displaced jet. In addition, the NEA mode tends to be related to the Eurasian teleconnection pattern, while the EA mode is associated with the East Asia–Pacific/Pacific–Japan pattern.

Key words: surface air temperature, Northeast Asia, East Asia, circulation anomaly, interannual variability

Citation: Chen, W., and Coauthors, 2016: Variation in summer surface air temperature over Northeast Asia and its associated circulation anomalies. *Adv. Atmos. Sci.*, **33**(1), 1–9, doi: 10.1007/s00376-015-5056-0.

1. Introduction

Great attention has been paid to the interannual variability of Northeast Asia (NEA) summer temperature, because of its effects on the economy (e.g., Ding, 1980; Sun et al., 1983). The variability in NEA summer temperature is related to a variety of atmospheric patterns. It was found that the pattern of wave trains along the upper-tropospheric westerly jet affects the NEA summer temperature (Sato and Takahashi, 2006). A Rossby wave pattern extending from the Indian Peninsula to NEA is associated with NEA temperature variability (Chen and Lu, 2014a). In addition, the East Asia–Pacific/Pacific–Japan (EAP/PJ) teleconnection pattern associated with convection over the tropical western North Pacific can also modulate the summer climate over NEA (Hirota and Takahashi, 2012; Chen and Lu, 2014a). In addition to the two above-mentioned factors, many other factors, including the Okhotsk highs (Sato and Takahashi, 2007), polar vortex (Zhang et al., 1985; Gu and Yang, 2006), Northern Hemisphere annular mode (He et al., 2006; Wang and Sun, 2009) and western North Pacific subtropical high (Cui et al., 2007), are also known to influence NEA summer temperature. The variety of teleconnection patterns mentioned above is indicative of the complexity of the remote circulations associated with NEA summer temperature variability.

It is expectable that the local circulation anomalies contribute to anomalous NEA temperature. In the middle troposphere, anomalous geopotential height over NEA affects the local summer temperature (Northeast China Cold Summer Research Group, 1979). If NEA is covered by negative height anomalies, cold air becomes active and flows southward from the high latitudes into NEA, resulting in a cold summer. On the other hand, positive height anomalies are associated with warmer NEA temperatures (Chen and Lu, 2014a). In the lower troposphere, an anticyclonic circula-

* Corresponding author: Riyu LU
Email: lr@mail.iap.ac.cn

tion anomaly occurs along with warming over NEA (Chen and Lu, 2014a; Gao et al., 2014). The strong southwesterly in the west of the anticyclonic circulation prevents the cold air in the high latitudes from flowing southward and results in a higher than normal temperature over NEA (Chen and Lu, 2014a).

Furthermore, climate variability over NEA exhibits a regional difference. Iwao and Takahashi (2006, 2008) indicated that the interannual variation of precipitation over NEA shows a seesaw pattern in the north and south of Lake Baikal. Sun and Wang (2006) pointed out that the interannual variability of temperature in Northeast China exhibits a seesaw pattern between its north and south areas, shown as the second dominant mode, while the first leading mode shows homogeneous variability in the whole region. Therefore, the temperatures in the north and south areas of Northeast China may exhibit significantly different variations. These studies suggested that the interannual variability of NEA summer temperature not only exhibits homogeneous variation, but also shows a regional difference in spatial distribution. Thus, what kind of modes does NEA temperature exhibit? What circulation patterns are associated with such temperature distributions? To answer these questions the present study investigates the dominant modes of interannual variability of NEA surface air temperature and its associated circulation anomaly during summer. The remainder of the paper is organized as follows: We introduce the datasets used in this work in section 2. In section 3, the two leading modes of NEA summer temperature are described. The different circulation patterns associated with these two modes are compared in section 4. And finally, conclusions are given in section 5.

2. Datasets

The present study uses Climatic Research Unit (CRU; Harris et al., 2014) surface air temperature data based on weather station records, and monthly mean ERA-Interim (European Centre for Medium-Range Weather Forecasts Interim Reanalysis) data (Dee et al., 2011) for the atmospheric circulation variables including geopotential height, temperature and wind fields. The study period is from 1979 to 2012. The mean of June, July and August (JJA) represents summer time. We highlight the interannual variability in this study and, considering that there is an appreciable decadal variation in NEA summer temperature (Sun and Wang, 2006; Chen and Lu, 2014b), obtain the component of interannual variability by applying a 9-year Gaussian filter. Statistics analysis is performed after the filtering of all datasets.

3. Leading modes of the summer temperature over NEA

Figure 1 shows the two leading modes of NEA summer temperature, obtained by performing EOF analysis on the summer surface air temperature anomaly within the region (30°–70°N, 100°–150°E). These two leading modes explain 50.8% of the total variance. The first leading mode (EOF_1) exhibits as a homogeneous temperature anomaly over NEA, extending from southeast of Lake Baikal to Japan and with

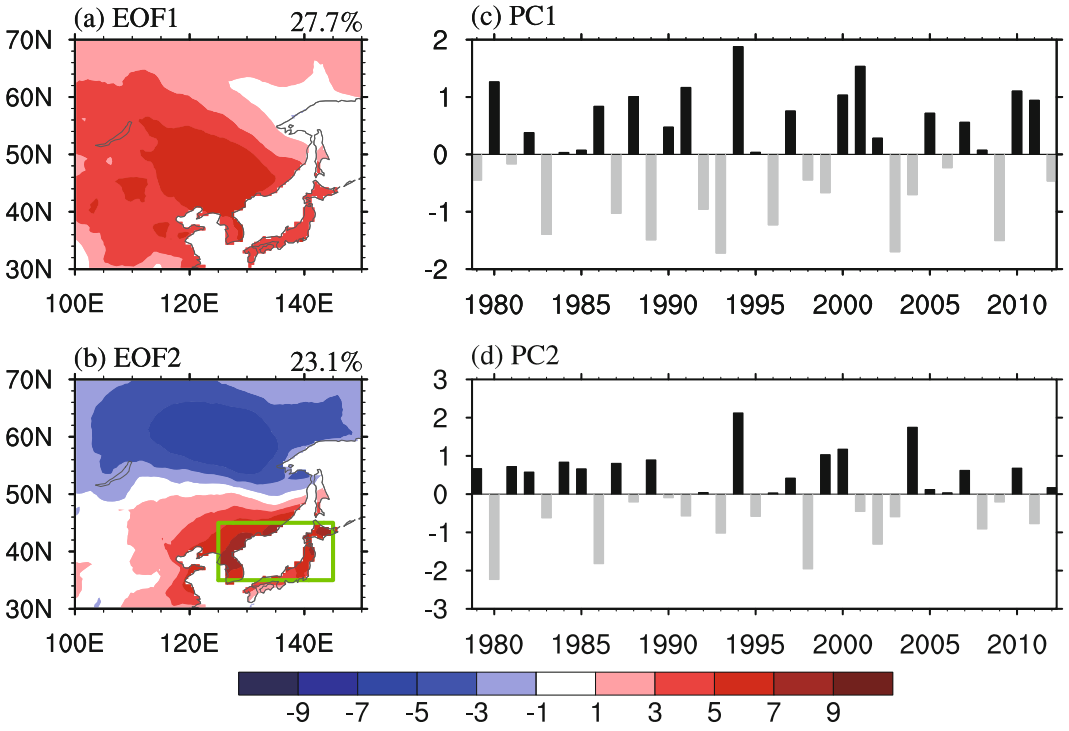

Fig. 1. The (a, c) first and (b, d) second leading modes and their PC time series for the summer surface air temperature over NEA, determined by EOF analysis.

a central area in Northeast China (Fig. 1a); the phase line of warm anomalies declines from northwest to southeast. This mode suggests a homogeneous change for the interannual variability of temperature over NEA, including the southeastern part of Russia, Mongolia, northern China, the Korean Peninsula and Japan. Thus, EOF_1 is named the NEA mode. This mode explains 27.7% of the total variance, which is dominant in NEA.

It should be mentioned that the time series for the first leading mode (PC1) shows a strong decadal variability, if the EOF analysis is performed using the original data (not shown). The decadal variance is so strong that it can explain more than half of the total variance (55.6%). Therefore, to highlight the interannual variability, we remove the decadal variations obtained by a 9-year Gaussian filter from the original data before performing the EOF analysis.

The second leading mode (EOF_2) behaves as a seesaw pattern for the temperature anomaly (Fig. 1b), in contrast with the homogeneous anomaly in EOF_1. A positive temperature anomaly and a negative anomaly are located south and north of 50°N, respectively. The positive anomaly is concentrated over EA, including the region of Changbai Mountains in Northeast China, the Korean Peninsula and central Japan. On the other hand, the negative temperature anomaly is over the northeast of Lake Baikal. EOF_2 displays an opposite temperature anomaly between south and north of NEA and explains 23.1% of the total variance. EOF_2 mainly contributes to a homogeneous temperature anomaly over EA, and is therefore called the EA mode. The seesaw pattern is similar to the distribution of the temperature anomaly associated with the Okhotsk highs in Sato and Takahashi (2007, Fig. 6b). Additionally, it should be noted that the seesaw pattern in this study is significantly different from the seesaw pattern indicated by Sun and Wang (2006). In their result, the seesaw pattern shows a contrasting distribution of temperature anomalies between south and north of 45°N, rather than the latitude of 50°N in this study. This difference results from the different domains for the EOF analysis: we investigated the whole NEA area, which is much larger than that in Sun and Wang (2006), whose study was based on 23 stations over Northeast China.

The surface temperature anomalies in 1980 and 2004, when a negative and a positive EA mode are dominant in NEA, respectively, are illustrated in Fig. 2. In 1980, there are negative temperature anomalies along the eastern border of Northeast China, over the Korean Peninsula and central Japan, and positive ones over other parts of NEA. This pattern is similar to the distribution of the temperature anomaly corresponding to the strong Okhotsk highs (Fig. 6b in Sato and Takahashi, 2007). Actually, the higher temperature in EA is contributed to by the frequent occurrence of the Okhotsk highs in summer 1980 (Kodama, 1997). The temperature pattern in 2004 is basically opposite to that in 1980, except for a positive anomaly near the southeast of Lake Baikal. These two years both show a seesaw pattern of the temperature anomaly, indicating a regional difference between the south and north of NEA. This figure confirms the existence

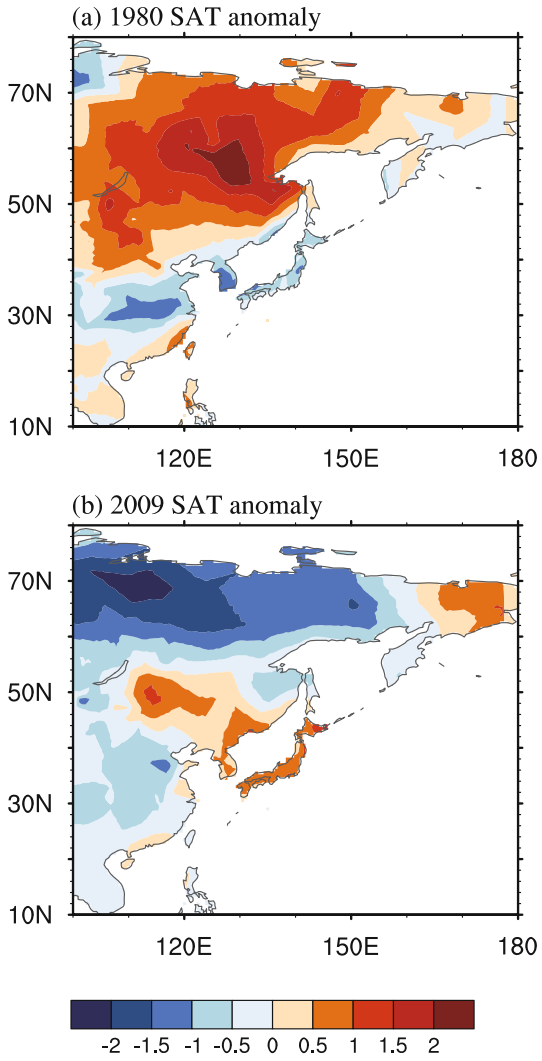

Fig. 2. The summer surface air temperature anomaly (units: °C) over NEA during (a) 1980 and (b) 2004.

of the EA mode.

Figure 3 shows the variance explained by these two modes in each grid box of NEA. PC1 contributes to the interannual variability of the temperature anomaly southeast of Lake Baikal (Fig. 3a). For most regions, the explained variance is more than 20%, including Mongolia, Northeast China, the Korean Peninsula and Japan. In central Northeast China, the explained variance is more than 40%. On the other hand, PC2 is in response to the temperature anomaly over the region of the Changbai Mountains, Korean Peninsula, Japan and northeast of Lake Baikal (Fig. 3b). The variance explained by PC2 in these regions is approximately 40%. Overall, the interannual variability of NEA temperature is modulated by these two modes (Fig. 3c). The temperature variances in EA can be mostly explained by these two modes, which together explain more than 60% of the total variance in most areas of EA. In particular, these two modes explain about 90% of the total variance in the Changbai Mountains.

Figure 4 shows the time series of the temperature anomaly over EA, defined as the East Asian Temperature

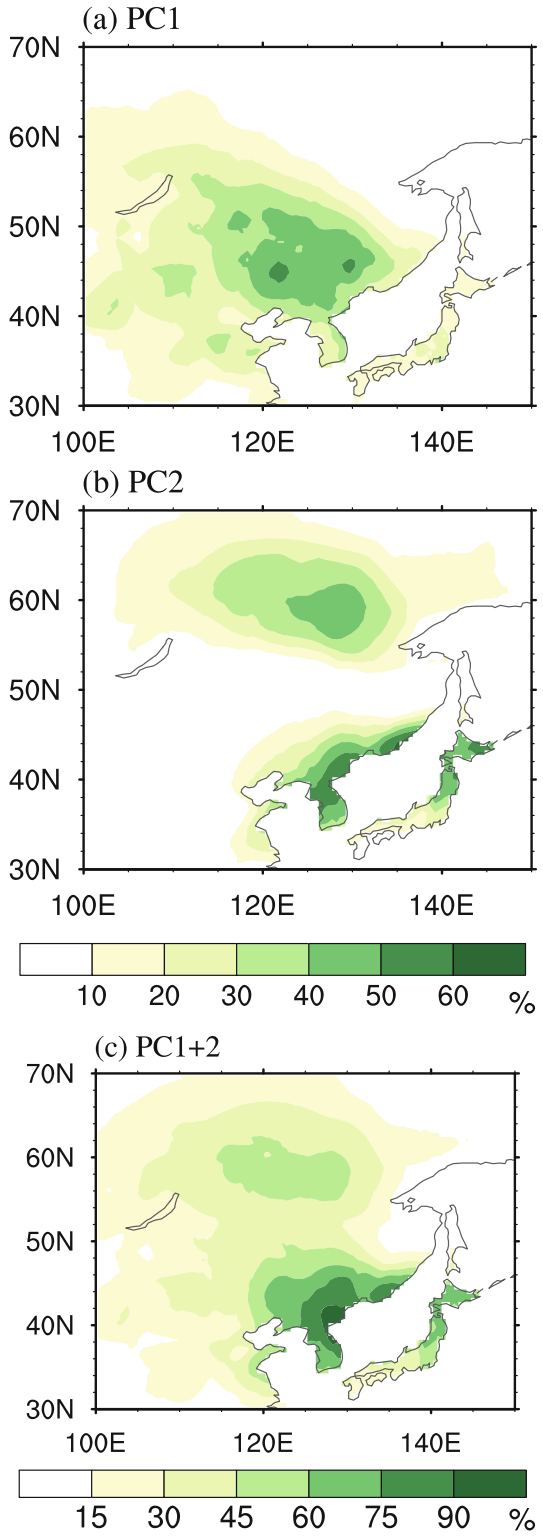

Fig. 3. The variance for each grid over NEA explained by (a) PC1, (b) PC2 and (c) PC1 and PC2 combined.

(EAT) index. The EAT index represents the temperature anomalies averaged over the region (35°–45°N, 125°–145°E). The EAT index is closely related with PC1 and PC2, with correlation coefficients of 0.62 and 0.57, respectively, both significant at the 99% confidence level. The similar coefficients suggest that the temperature anomalies in EA are equivalently affected by the NEA and EA modes, confirming the results shown in Fig. 3. Furthermore, the years when PC1 and PC2 are greater (less) than 0.8 (−0.8) standard deviation are marked. Half of the years (16 years) are dominated by only one mode: ten years by PC1 and six years by PC2. Seven years are dominated by the combination of PC1 and PC2. Among them, PC1 and PC2 offset each other in four years and overlap in other years. These results suggest that attention should be paid to both PC1 and PC2 for the temperature anomaly over EA.

Figure 5 shows the vertical profiles of temperature anomalies over NEA associated with these two modes. Along 125°–145°E, the NEA mode is characterized as a strong temperature anomaly in the midlatitudes (35°–55°N) (Fig. 5a). The temperature anomalies extend from the lower to the upper troposphere. On the contrary, the EA mode is related to a shallow temperature anomaly confined to the lower troposphere, but much weaker in the middle and upper troposphere. In the upper troposphere, there are some positive anomalies, which are mainly over the higher latitudes rather than the EA region (Fig. 5b). Additionally, the positive temperature anomaly around 40°N is associated with negative temperature anomalies in the higher and lower latitudes. Thus, in the meridional direction, the vertical structures for the summer temperature anomaly in response to these two modes are different. Furthermore, this difference can also be demonstrated in the zonal direction (Figs. 5c and d). Along 35°–45°N, the NEA mode shows a strong temperature anomaly covering 90°–150°E in the whole troposphere, but the EA mode shows a positive anomaly over 120°–150°E and is mainly limited to the lower troposphere. It seems that the vertical profile of the temperature anomaly associated with PC2 tends to be northward- and westward-tilted with height (Figs. 5b and d), implying the existence of local baroclinic energy conversion from mean flows to the EAP/PJ pattern (Kosaka and Nakamura, 2006; Chen et al., 2013).

4. Circulation associated with NEA summer temperature variability

These different temperature modes are associated with different circulation patterns. Figure 6 shows the 500 hPa geopotential height anomalies associated with the two PCs. For PC1, there is a remarkable positive geopotential height anomaly over NEA, with a central area in Northeast China. This positive anomaly covers the whole of NEA and is accompanied by warmer temperatures (Fig. 1a). Furthermore, this positive anomaly is related to a negative and a positive anomaly over the north of the Caspian Sea and near the Scandinavian Peninsula, respectively, corresponding to the Eurasian teleconnection (EU) pattern (Wallace and Gutzler, 1981). The correlation coefficient between PC1 and the EU index (Wallace and Gutzler, 1981) is 0.47, significant at the 99% confidence level. Moreover, the wave activity flux shown in Fig. 6a indicates that the EU teleconnection pattern

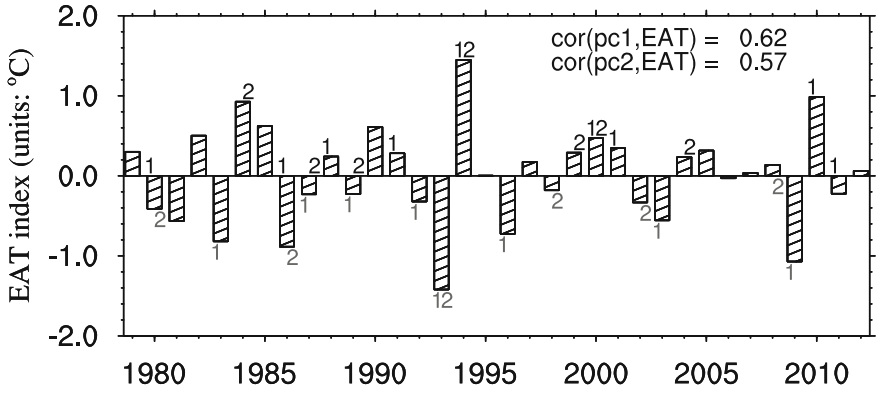

Fig. 4. The time series of the EAT index (units: °C), defined as the surface air temperature averaged within the region (35°–45°N, 125°–145°E), marked in Fig. 1. The years when PC1 and PC2 are greater (less) than 0.8 (−0.8) standard deviation are marked.

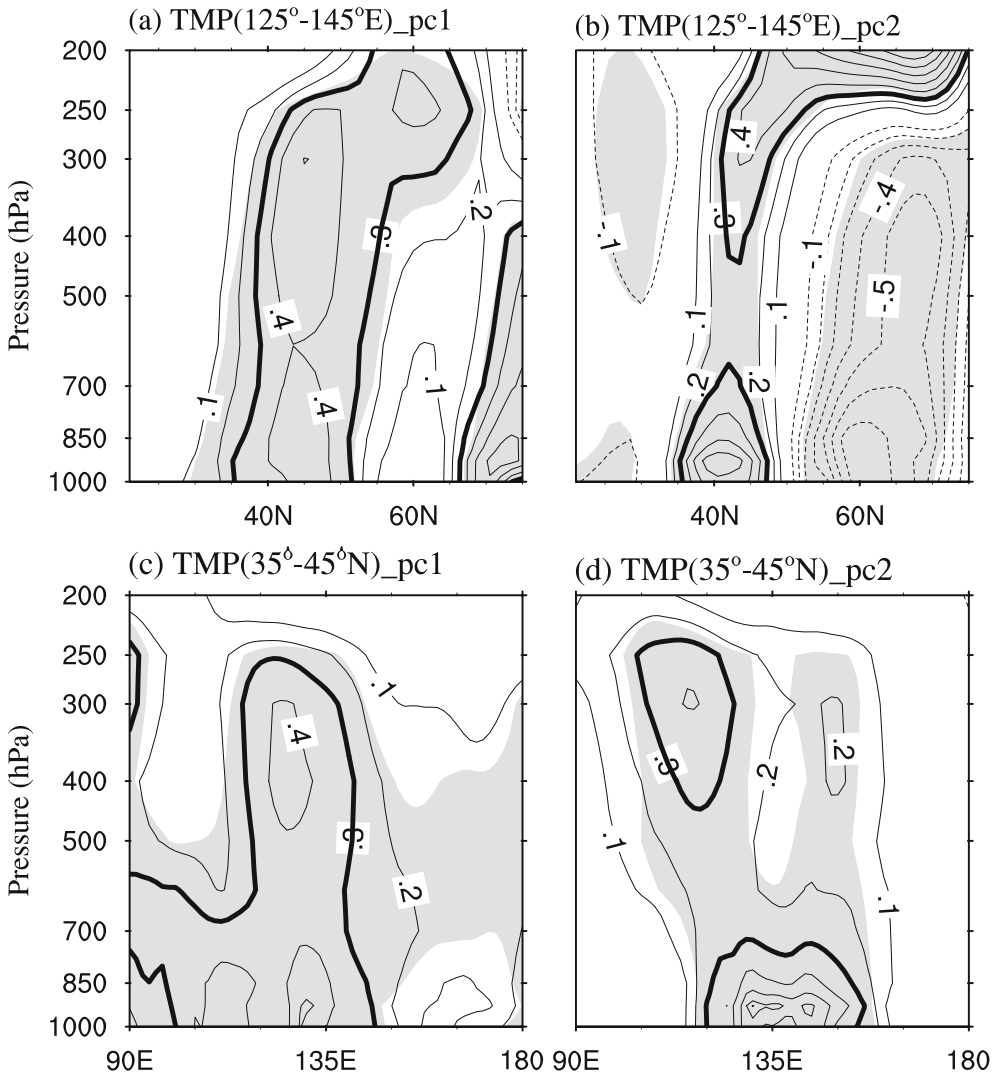

Fig. 5. Regression of the vertical profile of temperature anomalies (units: °C) onto the (a, c) first and (b, d) second PC time series: (a, b) temperature anomalies averaged over 125°–145°E; (c, d) temperature anomalies over 35°–45°N. Shading indicates regions where anomalies are significant at the 95% confidence level, according to the *t*-test. The thick contours represent 0.3°C.

can be considered as the eastward propagation of planetary waves from Western Europe to NEA, and can contribute to the NEA mode. These circulation anomalies associated with the NEA mode are different from those in Sato and Takahashi (2006), who suggested that a wave train along the westerly jet affects the summer temperature in Japan.

For PC2, however, the positive geopotential height anomaly is weaker and southward shifted, being limited to EA. It is associated with negative anomalies over the northeast of Lake Baikal. The seesaw pattern of the geopotential height anomaly corresponds to a similar pattern for the temperature anomaly (Fig. 1b). Additionally, it is also related to a negative anomaly over the western North Pacific. This distribution of circulation anomalies resembles the EAP/PJ pattern (e.g., Nitta, 1987; Huang and Sun, 1992). Additionally, the wave activity flux shown in Fig. 6b indicates that the EAP/PJ teleconnection is characterized by a connection among higher, middle and lower latitudes (e.g., Nitta, 1987). The correlation coefficient between PC2 and the EAP index (Huang and Yan, 1999) is 0.82. Huang and Yan (1999) defined the EAP index by the 500 hPa geopotential height anomaly at 40°N minus that at 20°N and 60°N, along the longitude of 125°E. This close relationship between the EA mode and EAP pattern implies that the EA mode may be related to the convection anomalies in the tropical western North Pacific, since it is well-known that the EAP/PJ pattern is closely associated with tropical convection anomalies. Actually, a positive (negative) EA mode is significantly associated with significantly enhanced (suppressed) convection over the Philippine Sea, which is not shown, but can be illustrated by the high correlation coefficient (-0.74) between PC2 and the outgoing longwave radiation anomaly over the Philippine Sea (10°–25°N, 120°–140°E). This EAP/PJ pattern is similar to that in Hirota and Takahashi (2012, Fig. 4b). Hirota and Takahashi (2012) suggested that the EAP/PJ pattern is an internal mode in the atmosphere, but can be affected by the convection activity over the tropical western North Pacific. Therefore, we suggest that the EA mode can also be considered as an internal mode, but is affected by tropical forcing.

The temperature anomaly for the NEA mode is mainly contributed to by the local geopotential height anomaly (Chen and Lu, 2014a; Gao et al., 2014). The positive anomaly southeast of Lake Baikal (Fig. 6a) is closely related to the warm temperature over NEA (Fig. 3a). On the other hand, the positive geopotential height anomaly associated with the EA mode (Fig. 6b) is relatively weak, and its contribution to the temperature anomaly in EA may be small.

The differences between the circulation patterns associated with two PCs can also be illustrated by the profiles of geopotential height (Fig. 7). The profile of geopotential height associated with PC1 shows a strong positive center in

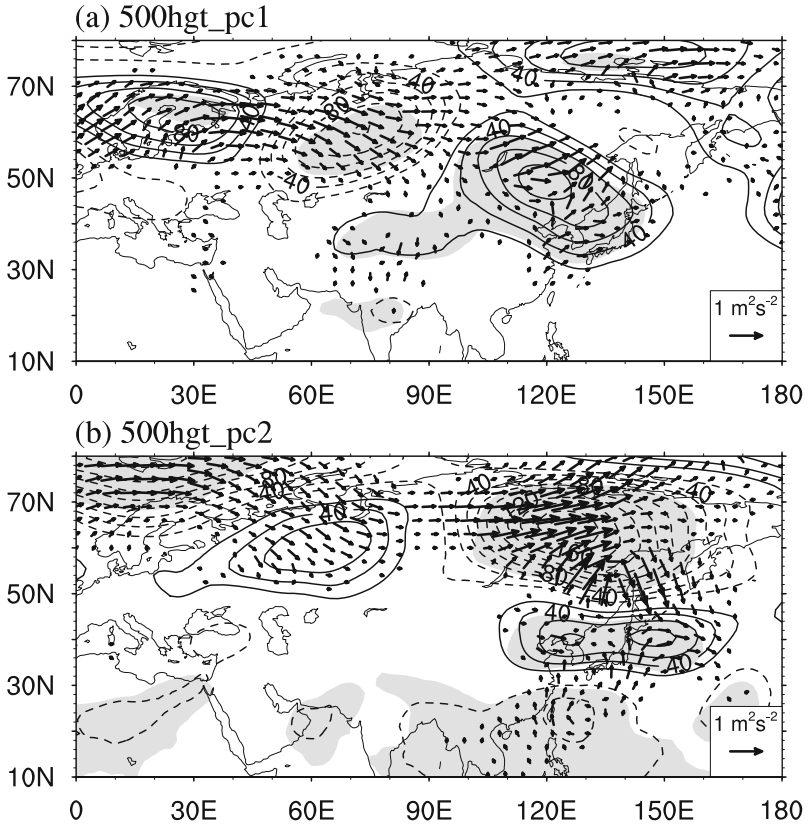

Fig. 6. As in Fig. 5 but for the 500 hPa geopotential height anomaly (units: m) and stationary wave activity flux [vectors; units: $m^2\ s^{-2}$; according to Takaya and Nakamura (2001)].

middle latitudes (Fig. 7a). This anomaly extends from the upper to lower troposphere, being consistent with the deep temperature anomaly over NEA (Figs. 5a and c). In addition, the positive anomaly seems to be isolated in the meridional direction, without connection with the lower and higher latitudes. On the contrary, PC2 is associated with a narrow positive center in the middle latitudes, and shows a "$+-+$" pattern from the lower to higher latitudes (Fig. 7b), indicating a connection of the EA mode with the lower and higher latitudes.

Figure 8 shows the zonal wind anomalies at 200 hPa associated with the NEA and EA modes. The NEA mode is associated with a negative anomaly along 40°N where the climatological East Asian jet (EAJ) locates. Therefore, the NEA mode is related to the change in the intensity of the EAJ. PC1 is significantly correlated with the EAJ intensity index, with a negative correlation coefficient of -0.58. Here, we define the EAJ index as the 200 hPa zonal wind anomalies averaged over (35°–45°N, 100°–140°E), which is similar to Lu (2004)

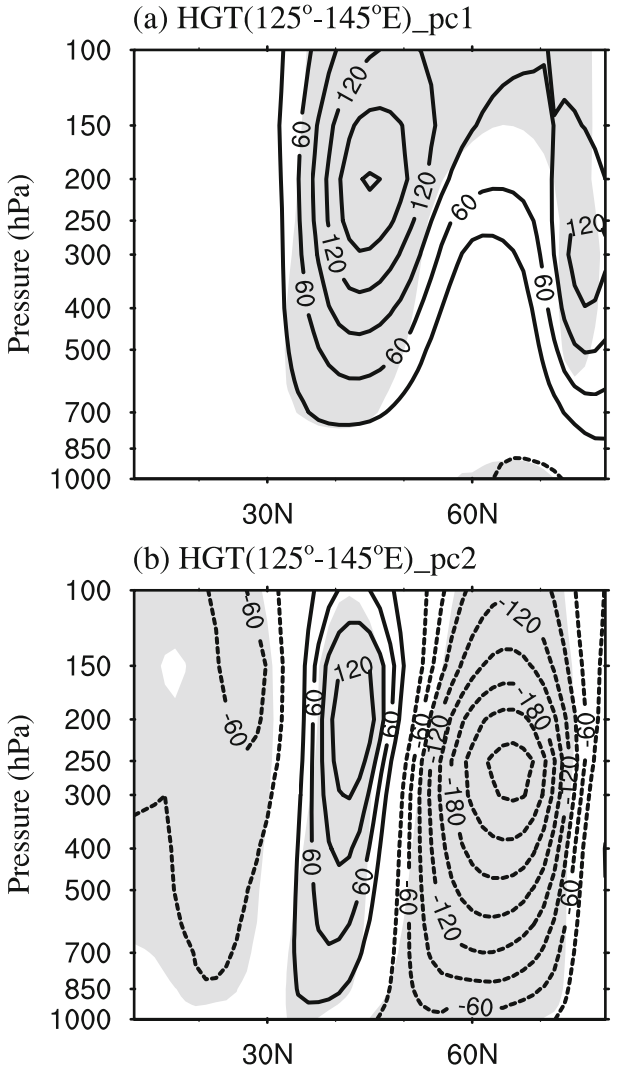

Fig. 7. As in Fig. 5 but for the vertical profile of the geopotential height anomaly averaged over 125°–145°E (units: m).

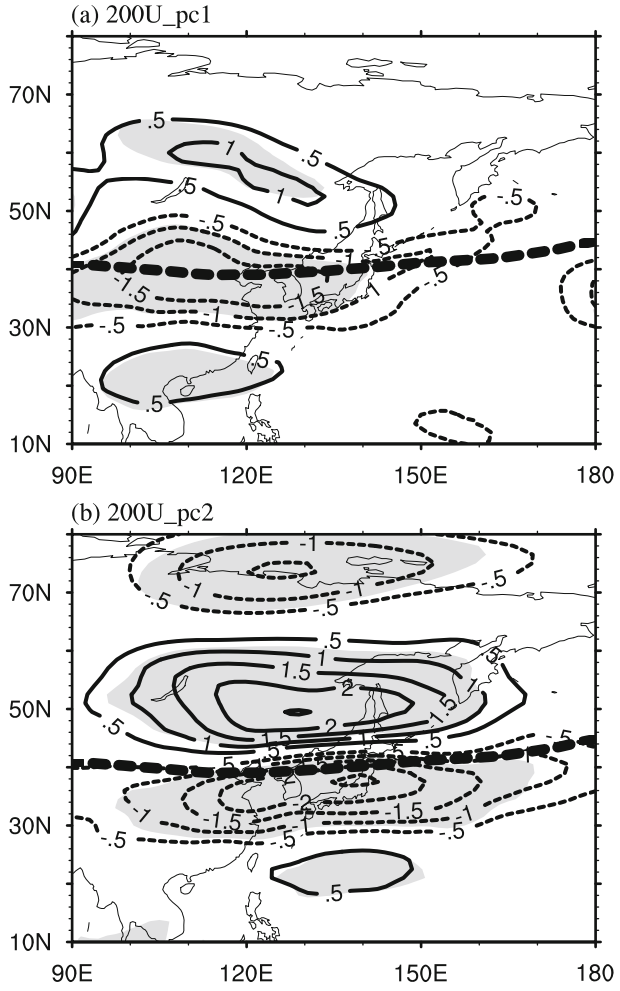

Fig. 8. As in Fig. 5 but for the 200 hPa zonal wind anomaly (units: m s^{-1}). The thick dashed lines represent the location of the climatological East Asian westerly jet.

but with a westward shift of the averaging region. The results suggest that a warm (cold) NEA mode corresponds to a weakened (strengthened) EAJ. The connection between the NEA mode and the EAJ intensity can be explained by the weakened meridional gradient of geopotential heights over the EA in association with the positive height anomaly over NEA (Fig. 6a).

On the other hand, PC2 is associated with a positive anomaly and a negative one north and south of the EAJ, respectively (Fig. 8b). It means that the EA mode is related to a meridional shift of the EAJ. Furthermore, the correlation coefficient between PC2 and the EAJ meridional shift index is 0.69. The EAJ meridional shift index is defined as the difference of 200 hPa zonal wind anomalies averaged over (40°–50°N, 100°–140°E) and (30°–40°N, 100°–140°E), which is similar to Lu (2004) and Lin and Lu (2005) but with a westward shift of the averaging regions. These results indicate that a positive (negative) EA mode is in response to a northward (southward) shift of the EAJ. The northward (southward) shift of the EAJ is associated with an anticyclonic (a cyclonic) anomaly (Fig. 6b) and a warmer (colder) tempera-

ture in EA (Fig. 1b).

5. Conclusions

This study investigates the two leading modes of interannual variation of summer surface temperature over NEA during the period 1979–2012. EOF analysis is applied on NEA summer temperature using CRU data, which are based on weather station records.

Two leading modes are demonstrated in this study. The first leading mode is characterized as the NEA mode, with a homogeneous temperature anomaly covering the whole of NEA. This mode indicates a homogeneous change in the interannual variability of summer temperature extending from southeast of Lake Baikal to Japan. The second leading mode exhibits as a seesaw pattern between the following two regions: (1) the Changbai Mountains in Northeast China, the Korea Peninsula and central Japan; and (2) northeast of Lake Baikal. This mode is called the EA mode. These two modes are associated with different vertical structures of temperature: significant air temperature anomalies appear in the entire troposphere for the NEA mode, but are concentrated in the lower troposphere for the EA mode.

Moreover, both modes are equivalently important to the temperature over the region of the Changbai Mountains, Korean Peninsula and central Japan. The correlation coefficients between PC1 and PC2 with the temperature averaged over this region are 0.62 and 0.57, respectively. The interannual variance of temperature over EA explained by the NEA mode is close to that explained by the EA mode. Thus, the results indicate that EA temperature is modulated by the combination of these two modes.

The two leading modes are in response to different patterns of circulation anomalies. The warm NEA mode is related to a strong positive geopotential height anomaly over NEA in the entire troposphere, while the warm EA mode is associated with a positive height anomaly over EA and a strong negative anomaly to the north. Correspondingly, the warm NEA mode is associated with a weakened upper-tropospheric westerly jet, and the warm EA mode is related to a poleward shifted westerly jet. In addition, the NEA mode tends to be related to the EU pattern, while the EA mode is closely related to the EAP/PJ pattern.

The present results suggest that the regional difference in interannual temperature variability in NEA should be noticed besides the homogeneous change. The homogeneous change (the NEA mode) and regional difference (the EA mode) are in response to different circulation patterns and different physical processes. In particular, both modes contribute equivalently and greatly to the temperature anomalies over EA, suggesting that these modes should be further studied for a better understanding of temperature variability in EA.

Acknowledgements. The authors acknowledge the two anonymous reviewers for their valuable comments and suggestions. This study was supported by the National Natural Science Foundation of China (Grant Nos. 41105046 and 41320104007).

REFERENCES

Chen, G. S., R. H. Huang, and L. T. Zhou, 2013: Baroclinic instability of the silk road pattern induced by thermal damping. *J. Atmos. Sci.*, **70**, 2875–2893.

Chen, W., and R. Y. Lu, 2014a: The interannual variation in monthly temperature over Northeast China during summer. *Adv. Atmos. Sci.*, **31**(4), 515–524, doi: 10.1007/s00376-013-3102-3.

Chen, W., and R. Y. Lu, 2014b: A decadal shift of summer surface air temperature over Northeast Asia around the mid-1990s. *Adv. Atmos. Sci.*, **31**(4), 735–742, doi: 10.1007/s00376-013-3154-4.

Cui, J., J. Li, A. Z. Zhang, and Q. Yan, 2007: Advances in studies of summer low temperature in Northeast China. *Meteorologica Monthly*, **33**(4), 3–9, doi: 10.3969/j.issn.1000-0526.2007.04.001. (in Chinese)

Dee, D. P., and Coauthors, 2011: The ERA-Interim reanalysis: Configuration and performance of the data assimilation system. *Quart. J. Roy. Meteor. Soc.*, **137**, 553–597, doi: 10.1002/qj.828.

Ding, S. S., 1980: The climatic analysis of low temperature in summer over the Northeast China and influence for agricultural product. *Acta Meteorologica Sinica*, **38**(3), 234–242. (in Chinese)

Gao, Z. T., Z. Z. Hu, B. Jha, S. Yang, J. S. Zhu, B. Z. Shen, and R. J. Zhang, 2014: Variability and predictability of Northeast China climate during 1948–2012. *Climate Dyn.*, **43**, 787–804.

Gu, S. N., and X. Q. Yang, 2006: Variability of the northern circumpolar vortex and its association with climate anomaly in China. *Scientia Meteorologica Sinica*, **26**(2), 135–142. (in Chinese)

Harris, I., P. D. Jones, T. J. Osborn, and D. H. Lister, 2014: Updated high-resolution grids of monthly climatic observations–the CRU TS3.10 Dataset. *International Journal of Climatology*, **34**, 623–642. doi: 10.1002/joc.3711.

Hirota, N., and M. Takahashi, 2012: A tripolar pattern as an internal mode of the East Asian summer monsoon. *Climate Dyn.*, **39**, 2219–2238.

He, J. H., Z. W. Wu, and L. Qi, 2006: Relationships of Northern Hemispheric annual mode and Northeast China cold vortex with summer precipitation in East Asia and China. *Journal of Meteorology and Environment*, **22**, 1–5. (in Chinese)

Huang, G., and Z. W. Yan, 1999: The East Asian summer monsoon circulation anomaly index and its interannual variations. *Chinese Science Bulletin*, **44**(14), 1325–1329.

Huang, R. H., and F. Y. Sun, 1992: Impact of the tropical western Pacific on the East Asian summer monsoon. *J. Meteor. Soc. Japan*, **70**, 243–256.

Iwao, K., and M. Takahashi, 2006: Interannual change in summertime precipitation over northeast Asia. *Geophys. Res. Lett.*, **33**, L16703, doi: 10.1029/2006GL027119.

Iwao, K., and M. Takahashi, 2008: A precipitation seesaw mode between Northeast Asia and Siberia in summer caused by Rossby waves over the Eurasian Continent. *J. Climate*, **21**, 2401–2419.

Kodama, Y. M., 1997: Airmass transformation of the Yamase airflow in the summer of 1993. *J. Meteor. Soc. Japan*, **75**, 737–

751.

Kosaka, Y., and H., Nakamura, 2006: Structure and dynamics of the summertime Pacific–Japan teleconnection pattern. *Quart. J. Roy. Meteor. Soc.*, **132**(619), 2009–2030.

Lin, Z. D., and R. Y. Lu, 2005: Interannual meridional displacement of the East Asian upper-tropospheric jet stream in summer. *Adv. Atmos. Sci*., **22**, 199–211, doi: 10.1007/BF02918509.

Lu, R. Y., 2004: Associations among the components of the East Asian summer monsoon system in the meridional direction. *J. Meteor. Soc. Japan*, **82**, 155–165.

Nitta, T., 1987: Convective activities in the tropical western Pacific and their impact on the northern hemisphere summer circulation. *J. Meteor. Soc. Japan*, **65**, 373–390.

Northeast China Cold Summer Research Group, 1979: A preliminary study on the long range forecasting of the cold/warm summer in Northeast China. *Acta Meteorologica Sinica*, **37**(3), 44–58.

Sato, N., and M. Takahashi, 2006: Dynamical processes related to the appearance of quasi-Stationary waves on the subtropical jet in the midsummer northern hemisphere. *J. Climate*, **19**, 1531–1544.

Sato, N., and M. Takahashi, 2007: Dynamical processes related to the appearance of the Okhotsk high during early midsummer. *J. Climate*, **20**, 4982–4994.

Sun, J. Q., and H. J. Wang, 2006: Regional difference of summer air temperature anomalies in Northeast China and its relationship to atmospheric general circulation and sea surface temperature. *Chinese Journal of Geophysics*, **49**, 588–598.

Sun, Y. T., S. Y. Wang, and Y. Q. Yang, 1983: Studies on cool summer and crop yield in Northeast China. *Acta Meteorologica Sinica*, **41**(3), 313–321. (in Chinese)

Takaya, K., and H. Nakamura, 2001: A formulation of a phase-independent wave-activity flux for stationary and migratory quasigeostrophic eddies on a zonally varying basic flow. *J. Atmos. Sci.*, **58**, 608–627.

Wang, H. J., and J. Q. Sun, 2009: Variability of northeast China river break-up date. *Adv. Atmos. Sci.*, **26**(4), 701–706, doi: 10.1007/s00376-009-9035-1.

Wallace, J. M., and D. S. Gutzler, 1981: Teleconnections in the geopotential height field during the northern hemisphere winter. *Mon. Wea. Rev.*, **109**, 784–812.

Zhang, S. Q., T. J. Yu, F. Y. Li, X. M. Wang, X. F. Wang, and W. M. Wu, 1985: Seasonal variation of Northern Hemisphere polar vortex area and associated intensity, and their association with the temperatures in Northeast China. *Scientia Atmospherica Sinica*, **9**, 178–185. (in Chinese)